Detailed characterization of a cyclophilin from the human malaria parasite *Plasmodium falciparum*

Matthew BERRIMAN and Alan H. FAIRLAMB[1]

Department of Biochemistry, Wellcome Trust Building, University of Dundee, Dundee DD1 5EH, Scotland

Cyclosporin (Cs) A has pronounced antimalarial activity *in vitro* and *in vivo*. In other organisms, the drug is thought to exert its effects either by inhibiting the peptidylprolyl *cis/trans* isomerase activity of cyclophilin (CyP) or by forming a CyP–CsA complex that inhibits the phosphatase activity of calcineurin. We have cloned and overexpressed in *Escherichia coli* a gene encoding a CyP from *Plasmodium falciparum* (PfCyP19) that is located on chromosome 3. The sequence of PfCyP19 shows remarkable sequence identity with human CyPA and, unlike the two previously identified CyPs from *P. falciparum*, PfCyP19 has no signal peptide or N-terminal sequence extension, suggesting a cytosolic localization. All the residues implicated in the recognition of the synthetic substrate *N*-succinyl-Ala-Ala-Pro-Phe-*p*-nitroanilide are conserved, resulting in characteristically high Michaelis–Menten and specificity constants ($K_m \gg 120\ \mu M$, $k_{cat}/K_m = 1.2 \times 10^7\ M^{-1} \cdot s^{-1}$ respectively). As the first line in the functional characterization of this enzyme, we have assessed its binding affinity for CsA. In accordance with its tryptophan-containing CsA-binding domain, PfCyP19 binds CsA with high affinity ($K_d = 13$ nM, $K_i = 6.9$ nM). Twelve CsA analogues were also found to possess K_i values similar to CsA, with the notable exceptions of Val^2-Cs ($K_i = 218$ nM) and Thr^2-Cs ($K_i = 690$ nM). The immunosuppressants rapamycin and FK506 were inactive as inhibitors, consistent with other members of the CyP family of rotamases. The CsA analogues were also assessed as inhibitors of *P. falciparum* growth *in vitro*. Although their antimalarial activity did not correlate with inhibition of enzyme activity, residues 3 and 4 of CsA appeared to be important for inhibition of parasite growth and residues 1 and 2 for PfCyP19 inhibition. We propose that a malarial CyP–CsA complex presents residues 3 and 4 as part of an 'effector surface' for recognition by a downstream target, similar to the proposed mechanism for T-cell immunosuppression.

INTRODUCTION

Cyclophilins (CyPs) are a family of highly conserved proteins that are ubiquitously distributed across all organisms examined to date. CyP was originally identified as a cytosolic binding protein for the potent immunosuppressive drug cyclosporin (Cs) A [1]. Independently, CyP was found to have peptidylprolyl *cis/trans* isomerase (PPIase or rotamase) activity [2,3] as a result of a search for an enzyme that catalyses the slow *cis–trans* isomerization of prolyl imide bonds in peptide chains during protein folding [4].

CyPs catalyse the folding of small polypeptides and proteins *in vitro* and there is evidence that they also function as folding catalysts *in vivo* (reviewed in [5]). In addition, a *Drosophila* CyP-like protein, NinaA, functions as a chaperone *in vivo* by binding to an early folding intermediate of rhodopsin [6] and a similar putative chaperone function has been reported for the CyP-like domain of the nuclear pore component, RanBP2, in mammalian retinal cells [7]. Further evidence of a chaperone role has come from the analysis *in vitro* of the folding kinetics of carbonic anhydrase [8], although this finding has been disputed [9]. Increasingly, CyP family members are being identified which are components of large protein complexes, such as the steroid hormone receptor complex [10,11], suggesting that CyP may have a general function of mediating protein–protein interactions, utilizing their 'active sites' to bind specific proline-containing peptide sequences. Human CyP-A binds to Gag polyprotein in HIV-1 virions and provides an example of CyP and an endogenous partner protein that have been structurally characterized [12]. The CyP–Gag interaction is thought to have a role in either capsid dissociation or T-cell invasion [13], but is unlikely to involve protein folding [12].

Studies using yeast genetics have attempted to shed further light on the role of CyP by disrupting putative CyP encoding genes. A total of eight genes encoding CyP-like PPIases are present in the *Saccharomyces cerevisiae* genome [14]. All eight have now been disrupted both individually [14–17] and collectively [14]. Phenotypic changes have been observed upon disruption of *CPR1*, encoding a cytosolic CyP (resulting in resistance to CsA) [18], *CPR3*, encoding a mitochondrial CyP (causing a temperature-dependent inability to grow on lactate medium) [15], and *CPR7*, encoding a cytosolic CyP (resulting in an impaired rate of cell division) [16]. In contrast to a previous study, where *CPR4* was found to be essential [17], viable *cpr4* mutants have recently been reported [14]. Furthermore, the cumulative effect of multiple disruptions was equivalent to the sum of the individual phenotypes, arguing against redundancy between CyPs [14].

The immunosuppressive agent CsA was originally isolated as an antifungal agent but it has been from studying its effects on T-cell activation that an alternative aspect of CyP function has been revealed. Although CsA potently inhibits the PPIase activity of CyP, the immunosuppressive effect arises from forming a complex with CyP. The complex inhibits the phosphatase activity of calcineurin [19], thus preventing the translocation to the nucleus of a subunit of NF-AT (nuclear factor of activated T-cells) [20] and consequently the transcription of several cytokine genes.

In addition to the immunosuppressive effect of CsA, the drug has an inhibitory activity against a number of pathogenic

Abbreviations used: CyP, cyclophilin; hCyP, human cyclophilin; Cs, cyclosporin; CN, calcineurin; MeBmt, 4-[(E)-2-butenyl]-4,*N*-dimethyl-L-threonine; suc-AAPF-pNA, *N*-succinyl-Ala-Ala-Pro-Phe-*p*-nitroanilide; PPIase, peptidylprolyl *cis/trans* isomerase.

[1] To whom correspondence should be addressed (e-mail ahfairlamb@bad.dundee.ac.uk).

The nucleotide sequence reported in this paper has been submitted to the EMBL/GenBank database with accession number U33869.

organisms (reviewed in [21]). One of these came to light more than a decade ago when attempts were made to potentiate malaria infections in mice using CsA to suppress host immunity. Surprisingly, the converse was seen, whereby CsA inhibited growth of rodent malaria *in vivo* [22,23]. In addition, CsA and non-immunosuppressive analogues have been reported as having pronounced antimalarial activity *in vitro* against the human malaria parasites *Plasmodium vivax* [24] and *P. falciparum* [23], where the appearance of early erythrocytic ('ring') stage parasites is particularly affected [25].

Although the mode of action of CsA against malaria is not known, in analogy with other systems, where a toxic drug–immunophilin complex is formed, CyP is an obvious potential target. The first step in our understanding of the mode of the antimalarial activity is a thorough understanding of potential receptor molecules for CsA. To date, a PPIase activity has been identified in *P. falciparum* crude extracts that is inhibited by CsA [26] and two malarial CyP genes have been cloned and the recombinant proteins partially characterized [27,28]. In the present study, we have identified a third gene in this CyP family (*CPR3*) and provide a detailed physical and biochemical characterization of the recombinant protein (PfCyP19). Its sensitivities to CsA and other inhibitors are presented and compared with inhibition *in vitro* of parasite growth and the implications of these results on the rational design of novel antimalarial chemotherapeutic agents, based on CsA, will be discussed.

MATERIALS AND METHODS

Materials

P. falciparum 3D7 parasites were kindly provided by Dr. D. Walliker (University of Edinburgh, West Mains Road, Edinburgh, U.K.) and a *P. falciparum* FCB1 cDNA library in λZAPII (Stratagene) was provided by Dr. A. A. Holder (National Institute for Medical Research, Mill Hill, London, U.K.). Blots of *P. falciparum* 3D7 chromosomal DNA on nylon membranes were generously provided by Dr. J. M. Foster as part of the Malarial Genome Project. All restriction enzymes were obtained from Promega, and chromatography media and columns were from Pharmacia. Cs analogues and FK506 were generously given by Novartis (Basel, Switzerland) and Fujisawa (Munich, Germany) respectively, and rapamycin was obtained from Calbiochem (Nottingham, U.K.). Stock solutions were prepared as described previously [26]. *P. falciparum* clone 3D7 was cultured *in vitro* in human A^+ erythrocytes in medium supplemented with human A^+ serum as described previously [29]. Cultures (10 ml) were grown in 100 ml tissue-culture flasks at 37 °C with vigorous shaking and gassed daily with 5% O_2/5% CO_2/90% N_2. Cultures at 5–10% parasitaemia were lysed with 0.2% (w/v) saponin and genomic DNA was isolated using the SDS/proteinase K method [30].

cDNA library screening

Peptide sequences for a number of CyPs were aligned and partially degenerate oligonucleotides designed for two highly conserved regions: QGGDFT and WLDGKHV. The primers were designed according to the codon usage of *P. falciparum* as follows: 5′-CAA GGW GGW GAT TTY AC-3′ and 5′-ACC AAY CTR CCW TTK GTR CAC-3′. The oligonucleotides (final concentration 1 μM) were added to a mixture containing 10 mM Tris/HCl, pH 8.3, 50 mM KCl, 1.5 mM $MgCl_2$, the four dNTPs (each 200 μM), 2.5 units of Taq DNA polymerase (Boehringer Mannheim) and 1 μg of *P. falciparum* 3D7 genomic DNA. The PCR was performed using the following cycle parameters: 94 °C for 1 min, 50 °C for 1.5 min, 72 °C for 2 min repeated for 30 cycles followed by one cycle of 94 °C for 2 min, 50 °C for 2 min and 72 °C for 5 min. A PCR product of the expected size (~ 200 bp) was purified. An aliquot (~ 50 ng) was radioactively labelled with [α^{32}P]dCTP using the Multiprime DNA labelling system (Amersham) and used to screen a λZAPII cDNA library (3×10^4 independent clones), according to the manufacturer's protocol. Hybridizations were performed on nitrocellulose filters at 42 °C in the presence of 50% (v/v) formamide, according to standard methods [30] and stringency washed three times in 1 × SSC (150 mM NaCl/15 mM trisodium citrate, pH 7.0) for 10 min at 60 °C.

Subcloning and sequencing

The recombinant λZAPII cDNA was converted to a pBluescript SK(−) phagemid by *in vivo* excision using the ExAssist/SOLR system (Stratagene). The cloned cDNA was sequenced via the dideoxy chain termination method using [α^{35}S]dATP and a modified T7 DNA polymerase (Sequenase, Amersham). A contiguous sequence was constructed using the DNAstar sequence analysis package (DNAstar Corporation, Madison, WI, U.S.A.) and analysed using the University of Wisconsin Genetic Computer Group (GCG) programs.

Chromosomal localization

The gene encoding PfCyP19 (*CPR3*) was excised from an expression construct (see following section) and radioactively labelled using the Rediprime DNA labelling system (Amersham). Hybridizations to the chromosomal blots were performed in a solution containing 1 M NaCl, 1% SDS, 100 μg·ml^{-1} denatured salmon sperm DNA and radioactively labelled *CPR3* at 60 °C overnight. The filters were washed at 60 °C in three changes of 0.2 × SSPE (30 mM NaCl/2 mM NaH_2PO_4/0.2 mM EDTA, pH 7.4)/0.1% (w/v) SDS for 15 min each and then exposed to autoradiographic film.

Expression in *Escherichia coli*

CPR3 was amplified from *P. falciparum* 3D7 genomic DNA using the following 5′ and 3′ end-specific primers, with unique *Nde*I and *Bam*HI restriction enzyme sites: 5′-gg ccc gcg cat ATG AGT AAG AGG AGT AAA GTT-3′ and 5′-cgc gga tcc TTA CAA TTC ACC ACA ATC AGT-3′. The primers (final concentration 1 μM) were added to a mixture of 10 mM Tris/HCl, pH 8.8/10 mM KCl/0.002% (v/v) Tween 20/1.5 mM $MgCl_2$ containing the four dNTPs (final concentration 200 nM), 3 units of ULTma DNA polymerase (Perkin–Elmer) and ~ 100 ng genomic DNA. The following cycle parameters were used for PCR: 94 °C for 1 min 45 s followed by 5 cycles of 94 °C for 45 s, 50 °C for 1 min, 72 °C for 1 min; 25 cycles of 94 °C for 45 s, 60 °C for 1 min, 72 °C for 1 min and 72 °C for 10 min. The PCR product was cloned into pCR-Script SK(+) (Stratagene) and used to transform *E. coli* strain JM109. Plasmid DNA was prepared (QIAprep, Qiagen) and the sequence confirmed by automated cycle sequencing using the dye terminator method (ABI PRISM dye terminator kit, Perkin–Elmer). *CPR3* was excised from the plasmid by *Nde*I and *Bam*HI digestion, purified from a 1% agarose gel (QIAEX II gel extraction kit, Qiagen), subcloned into pET-3a (Novagen) and used to transform *E. coli* JM109.

For expression, recombinant pET-3a.*CPR3* plasmid was prepared and *E. coli* BL21(DE3) strain was transformed. Single

colonies were picked and grown to mid-log phase ($D_{600} = 0.6$) at 37 °C in Luria-Bertani broth medium containing 50 $\mu g \cdot ml^{-1}$ ampicillin; isopropyl-β-D-thiogalactopyranoside was added (final concentration 0.4 mM) and the incubation continued for a further 3 h. Cells were harvested by centrifugation at 4500 ***g*** for 10 min at 4 °C, lysed by sonication and expression was monitored by SDS/PAGE in 15 % acrylamide gels. For purification, this procedure was scaled up to cultures of 2 l, and the cell pellets were stored at −20 °C until required.

Purification of recombinant PfCyP19

A frozen cell pellet of *E. coli* (wet weight, 6.9 g) was thawed in buffer A (20 mM Tris/HCl, pH 7.8), lysed by sonication and centrifuged at 15000 ***g*** for 20 min to remove cell debris. The supernatant was fractionated by addition of solid $(NH_4)_2SO_4$ and the precipitate formed between 40 and 60 % saturation was collected by centrifugation. The pellet was redissolved in buffer A and dialysed extensively against the same buffer (2 × 500 ml and 1 litre, overnight).

Further purification was carried out on a BioRad BioLogic LP system, using a modification of the method described by Bose et al. [31]. The dialysed sample (9 ml) was loaded on to a Q Sepharose FF column (1.6 cm × 10 cm) equilibrated with buffer A. Unbound material was eluted using the same buffer, pooled and then concentrated by ultrafiltration in a Centriprep 10 (Amicon). After dialysis overnight against 1 litre of buffer B [20 mM (Na^+) Mes, pH 6.5], the sample was loaded onto a SP Sepharose FF column (1.6 cm × 10 cm) equilibrated with buffer B. Protein was eluted using a linear gradient of NaCl (0–0.5 M). Fractions with a high protein concentration were analysed by SDS/PAGE and those that contained a product of the expected size were pooled and concentrated. The concentrated sample (1.6 ml) was then loaded on to a column (1.6 cm × 100 cm) of Sephadex G-50 equilibrated with buffer A containing 150 mM NaCl. Fractions containing PfCyP19 were pooled, concentrated and stored at 4 °C until use. All purification steps were performed at 4 °C. Flow rates of 1.0 and 0.5 $ml \cdot min^{-1}$ were used for ion-exchange and gel-filtration chromatography respectively.

Protein determination and amino acid sequencing

Throughout the purification, protein concentration was determined using the Bradford assay with BSA as standard. The final concentration of the homogeneous protein was also determined by total amino acid analysis by comparing the recovery of a 25 pg sample with that of a test peptide (Department of Biochemistry, University of Bristol, Bristol, U.K.).

N-terminal sequence analysis was performed by the Medical Research Council Protein Phosphorylation Unit at the University of Dundee (Dundee, Scotland, U.K.).

Assay for PPIase activity

PPIase activity was determined using the synthetic peptide substrate, *N*-succinyl-Ala-Ala-Pro-Phe-*p*-nitroanilide (suc-AAPF-pNA) (Sigma) in a chymotrypsin-coupled colorimetric assay developed by Fischer et al. [4]. Assays were performed to determine the effect of substrate concentration using an assay mixture (1 ml) containing 35 mM (Na^+) Hepes, pH 7.9, 25–1500 μM peptide substrate (from a 75 mM stock in DMSO) and 20 nM PfCyP19. The mixtures were allowed to equilibrate at 10 °C for 10 min before initiating the reaction by the addition of 5 mg of α-chymotrypsin (Boehringer Mannheim, 500 $mg \cdot ml^{-1}$ stock in 1 mM HCl) and the increase in absorbance (typically at 390 nm) was recorded at 0.2 s intervals for 5 min, using a Beckman DU-640 spectrophotometer with a temperature controlled cell. Depending on the substrate concentrations, changes in absorbance were measured at 390, 430, 440, 445, 450 or 455 nm. The mixing time (typically 5 s) was measured to allow data to be extrapolated and the proportion of substrate in the *cis* conformation to be calculated from the difference between the final and initial (at the extrapolated zero time) absorbance values. Molar absorption coefficients of pNA were calculated with wavelength scans of assay reactions and the amount of suc-AAPF-pNA in each assay was determined. In subsequent experiments, at various enzyme concentrations, 74 μM suc-AAPF-pNA was used and reactions were initiated with 0.5 mg of α-chymotrypsin. Data were fitted to an exponential curve by non-linear regression analysis using the GraFit package (Erithacus Software) to obtain apparent first-order rate constants (k_{app}). The net enzyme-catalysed rate constant (k_0) was calculated by subtraction of the spontaneous non-enzymic rate constant (k_{spont}).

Determination of a K_d for CsA

The binding of CsA to PfCyP19 was studied using a modification of the procedure described by Liu et al. [32] based on enhancement of intrinsic tryptophan fluorescence upon binding of CsA to PfCyP19. Fluorescence was measured (Hitachi F4500) at room temperature. Optimal conditions, determined by scanning, were an excitation wavelength of 289 nm and emission wavelength of 324 nm, which was in close agreement with the fluorescence emission maxima for hCyPA [32]. CsA [10 μM stock in 20 % (v/v) ethanol] was titrated against 314 nM PfCyP19 in 2 ml of assay buffer to give a final concentration of 0–600 nM CsA. Addition of solvent alone was found to have no effect under the assay concentrations used [< 1.5 % (v/v)].

Inhibitor studies against PfCyP19

Enzyme assays were performed essentially as above, except that the enzyme was preincubated for 10 min at 10 °C with various concentrations (0–160 nM) of CsA analogues, before addition of the substrate and incubation for a further 5 min followed by initiation of the reaction with 0.5 mg of α-chymotrypsin. Assays were also performed with FK506, rapamycin and several known antimalarial agents. Controls were assayed in the presence of solvent alone. IC_{50} and, where possible, K_i data were determined using non-linear regression analysis with the GraFit package.

Parasite growth inhibitor studies *in vitro*

In vitro growth in the presence of the CsA analogues was measured using an adaptation of a method developed by Makler et al. [33]. Briefly, the activity of parasite-specific lactate dehydrogenase (pLDH), which is capable of using 3-acetyl pyridine adenine dinucleotide as a coenzyme, was measured by coupling the reaction to Nitroblue Tetrazolium to form the formazan reduction product.

Parasites were grown as described above except that the medium was supplemented with 0.5 % (w/v) lipid-rich BSA (Albumax II, Gibco BRL) instead of 5–10 % (v/v) human serum. Cultured parasites were centrifuged at 2000 ***g*** for 2 min and the pellets were resuspended in fresh medium containing erythrocytes to a final 2 % haematocrit and 3 % parasitaemia. Aliquots of 100 μl were transferred to each well of sterile, flat-bottomed microtitre plates containing 100 μl of serially diluted drugs [final concentrations of 8–4000 nM in 1 % (v/v) ethanol]. At the concentration used, ethanol alone had no detectable effect on

parasite growth. The plates were incubated for 48 h at 37 °C in a candle jar [29]. Infected erythrocytes were lysed by transferring 50 μl aliquots to 4 vol. of deionized water for 10 min and 60 μl of lysate was transferred to microtitre plate wells containing a previously optimized [34] assay mixture: 50 μl buffer [200 mM Tris, pH 9.2, 400 mM lithium lactate, 4 % (v/v) Triton X 100, 2 mM 3-acetyl pyridine adenine dinucleotide], containing 10 μl diaphorase (130 units $\cdot$ ml^{-1}; Boehringer Mannheim) and 10 μl Nitroblue Tetrazolium (1 mg $\cdot$ ml^{-1}). The increase in absorbance was measured at 595 nm using a Thermomax microtitre plate reader (Molecular Devices) for 15 min at 25 °C. Initial rates were determined by visual inspection of the progress curves and IC_{50} valves were calculated for each drug, using the GraFit package.

RESULTS

Sequence analysis

Two degenerate oligonucleotide primers were used to amplify by PCR a single 195 bp DNA fragment corresponding to a highly conserved central region of the CyP gene. A *P. falciparum* cDNA library was screened with the PCR product and a single 668-bp clone was isolated and sequenced. This clone possessed a single 515-bp open reading frame which was termed *CPR3* (CsA sensitive proline rotamase). *CPR3* shows the characteristic biased codon usage and A/T content (69 % increasing to 90 % outside the open reading frame) previously reported for other *P. falciparum* genes [35].

Radioactively labelled *CPR3* was hybridized to two blots of *P. falciparum* 3D7 chromosomal DNA, containing chromosomes 11–14 on one and chromosomes 1–10 on the other. After high stringency washing, the probe hybridized to the membrane with a high intensity signal corresponding to a low-molecular-mass chromosome and with lower intensity signals for two higher-molecular-mass chromosomes (results not shown). The high intensity signal was probably specific for hybridization to *CPR3*. Re-hybridizing the blot with the *P. falciparum* circumsporozoite protein (CSP) gene confirmed the localization as chromosome 3. It is likely that the two lower intensity signals represent hybridizations to *CPR1* and *CPR2*. A BLASTN search of the *P. falciparum* genome project at the Sanger Centre has subsequently identified a 20.5 kb contiguous sequence (PFSC03030) from chromosome 3 as identical with the complete *CPR3* cDNA sequence between nt 14491 and 15156.

A theoretical translation of *CPR3* indicates a protein of M_r 18.954, which has been termed PfCyP19 following nomenclature described previously [36]. Peptide sequences for PfCyP19 and 38 other CyP sequences were aligned using the program CLUSTAL and the PAM250 residue weighting matrix and a selection are shown in Figure 1. PfCyP19 has 67.7 % and 60.1 % sequence identity with the two *P. falciparum* CyPs (referred to here as PfCyP22 [27] and PfCyP24 [28]) reported previously. The percentage similarity was even higher for a large number of other sequences including, an M_r 20000 CyP from another apicomplexan parasite *Toxoplasma gondii* (TgCyP20, 78.2 %), a tomato CyP (73.4 %) and *S. cerevisiae* CyPA (71.2 %). Human CyPs (excluding large and complex CyPs such as hCyP40 and hCyP60) have sequence identities of 65.9 to 72.1 %, ranking them in the order: hCyPA > hCyPD > hCyPB > hCyPC. PfCyP22 and PfCyP24 have identities of between 59.6 % and 64.8 % with human CyPs. Over its entire length, PfCyP19 and other CyPs are highly conserved, which is consistent with an important, even if not vital, function in the cell. The alignment also reveals very high conservation of residues important for enzymic activity and for binding to CsA (Figure 1). The 13 residues that define a CsA binding pocket in the crystal structure of a hCyPA–CsA complex [37] are identical, including the single tryptophan that is essential for CsA binding [32]. Furthermore, the crystal structure of hCyPA complexed with suc-AAPF-pNA implicates 12 residues in binding the *cis* conformation of the substrate [38]. All 12 residues are identical in PfCyP19.

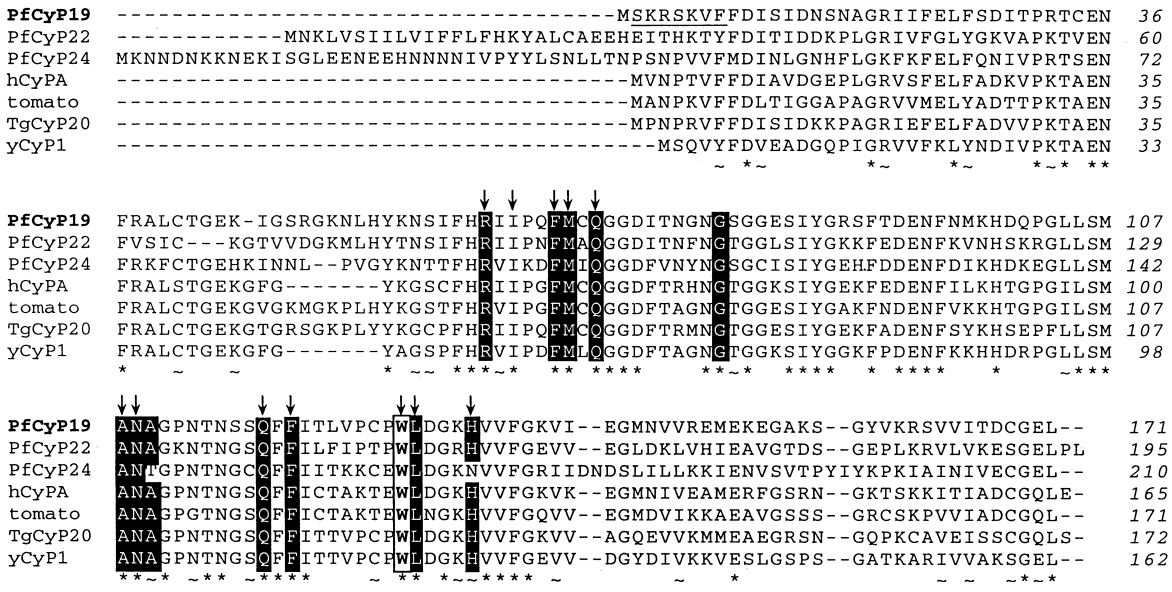

Figure 1 Clustal alignment of the sequence of PfCyP19 with related CyPs

Residues that are identical (*) or conserved (~) are indicated below the alignment. The tryptophan essential for CsA binding [32] is shown in bold and boxed and the twelve other residues important for CsA binding [37] are white on black. Arrows above the alignment indicate residues that are involved in binding suc-AAPF-pNA [38]. The amino acids determined by N-terminal sequence analysis are underlined. The sequences shown are from *P. falciparum*, PfCyP22 (X85956) and PfCyP24 (U10322); human, hCyPA (A94496); tomato CyP (P21568); *T. gondii*, TgCyP20 (U04634) and *S. cerevisiae*, yCyPA (X17505).

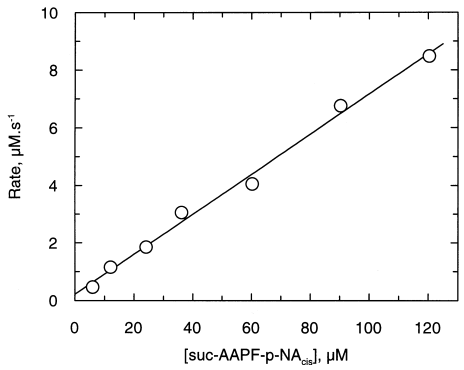

Figure 2 Initial reaction velocity of PfCyP19 PPIase activity with suc-AAPF-pNA

The initial reaction velocity as a function of the concentration of the *cis* conformation is shown.

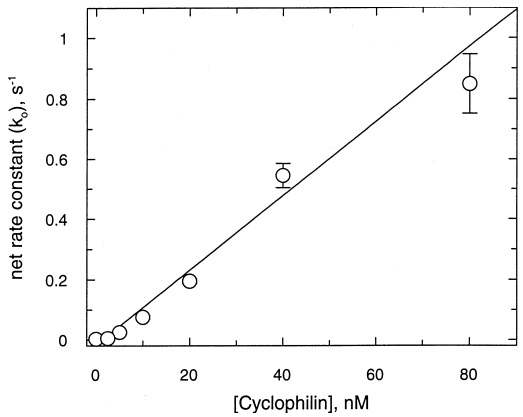

Figure 3 PPIase activity of purified recombinant PfCyP19

The net first-order rate constants (k_0) for the *cis–trans* isomerization of suc-AAPF-pNA as a function of PfCyP19 are shown. The line was fitted by linear regression with the gradient equivalent to k_{cat}/K_m. Each point represents the mean ± S.E. of three determinations.

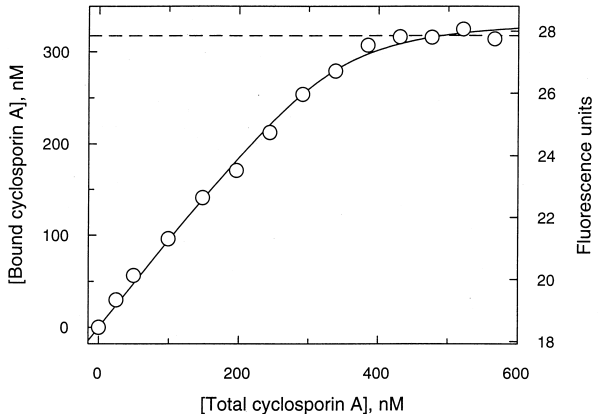

Figure 4 Enhancement of tryptophan fluorescence of PfCyP19 upon binding of CsA

The change in absolute fluorescence of 314 nM PfCyP19 upon titration with increasing CsA is shown (right axis). Using the assumption that maximum fluorescence (broken line) is due to 100% occupancy of the active site by CsA, corresponding values of bound drug (left axis) were calculated for each absolute fluorescence reading.

Expression and purification of PfCyP19

The entire coding region of *CPR3* and additional *Nde*I and *Bam*HI restriction sites were amplified by PCR from genomic DNA from *P. falciparum*, clone 3D7. The sequence was identical with that obtained from the cDNA library from strain FCB1, indicating that the gene does not contain any introns. The amplified gene was cloned into pET3A and used to transform an inducible expression host strain of *E. coli* bearing the T7 polymerase gene in its genome. After induction, bacterial extracts were analysed by SDS/PAGE and Coomassie Blue staining. Approx. 40 % of total soluble protein was of the expected M_r for PfCyP19 (approx. 19000).

The recombinant PfCyP19 was purified to a single band of M_r 19000, as assessed by SDS/PAGE (results not shown), using a combination of $(NH_4)_2SO_4$ precipitation, anion- and cation-exchange chromatography and gel-filtration chromatography. A linear NaCl gradient was used to elute protein from the S Sepharose (cation-exchange) column. One major peak eluted at approx. 0.35 M NaCl, which had been found previously during the purification of bovine endoplasmic reticulum-specific CyP [31]. The addition of a gel-filtration chromatography purification step was necessary to remove high-molecular-mass contaminants, which were visible on an overloaded SDS/polyacrylamide gel.

N-terminal sequence analysis yielded the first seven amino acids (excluding the initiator methionine) predicted from the gene sequence (Figure 1), confirming that the recombinant protein was correctly expressed. From the primary amino-acid sequence, an absorption coefficient of 10130 $M^{-1} \cdot cm^{-1}$ was calculated.

Biochemical properties of PfCyP19

In assays for PPIase activity, low concentrations of the chromogenic substrate suc-AAPF-pNA were used and it was assumed that the substrate concentration (S) $\ll K_m$ [2]. However, to date only the K_m for hCyPA (0.87 mM) has been reported [39]. To determine whether this was true for PfCyP19, PPIase activity was measured using 25–1500 μM suc-AAPF-pNA (Figure 2). The concentration of suc-AAPF-pNA in the *cis* conformation was determined using the experimental absorption coefficients and the difference between the initial and final absorbance values. The proportion of substrate in the *cis* conformation was 12.1 %, a number in close agreement with previous reports using an aqueous assay system [4]. Molar absorption coefficients ($M^{-1} \cdot cm^{-1}$) were calculated from at least three wavelength scans and the mean values at each wavelength (shown in parentheses) were as follows: 503 (455 nm), 794 (450 nm), 1229 (445 nm), 1808 (440 nm), 3611 (430 nm) and 13526 (390 nm). Over the range of substrate concentrations used, the data fitted well to a single exponential giving first-order progress curves and the corresponding reaction velocity, v, against substrate concentration (S) plot was linear (Figure 2). As discussed in [39], at substrate concentrations approaching the K_m, the spontaneous, uncatalysed isomerization would contribute increasingly to the initial velocity and the data would no longer fit a first-order analysis. This implies that, at 74 μM substrate ($cis \approx 9$ μM) which was used in subsequent assays, the assumption that $S \ll K_m$ is correct. Therefore the Michaelis–Menten equation can be simplified to $v = k_{cat}ES/K_m$. Since $v = k_0S$, the equation can be simplified further to $k_0 = k_{cat}E/K_m$. Thus a plot of k_0 versus E yields a k_{cat}/K_m of $(1.2 \pm 0.1) \times 10^7$ $M^{-1} \cdot s^{-1}$ for PfCyP19 (Figure

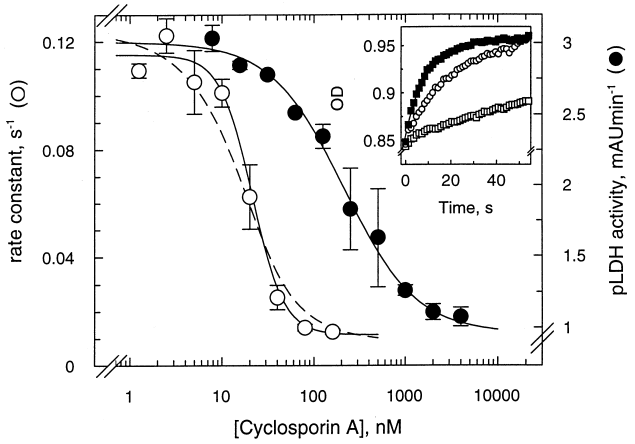

Figure 5 Effect of CsA on PPIase activity and parasite growth

Data represents the means ± S.D. for three determinations. Dose-response curve for inhibition of PPIase activity by CsA (○). The broken line indicates the approx. $K_{i,app}$ fit produced by applying eqn. (1) to the data. Effect on parasite growth, measured by parasite-specific lactate dehydrogenase activity (●). The inset shows the progress curves of a typical inhibition experiment with 20 nM PfCyP19 in the absence (■) or presence (○) of the IC_{50} concentration (20 nM) of CsA. Background spontaneous isomerization of suc-AAPF-pNA (□).

3), which is in agreement with previously published values for hCyPA, (1.4×10^7 to 2.2×10^7 $M^{-1} \cdot s^{-1}$ [40,41]).

The enhanced fluorescence of the single tryptophan residue of PfCyP19 upon CsA binding was used to study the interaction with PfCyP19. The binding of CsA to PfCyP19 approached the tight binding limit, indicated by the linear fit of the titration curve until near saturation was reached (Figure 4). Assuming that 100% occupancy had been reached at the maximum fluorescence, each absolute fluorescence value was converted in to the corresponding amount of bound CsA and a K_d of 13.0 ± 2.7 nM was calculated by fitting the data to the 'bound against total' equation of the GraFit package.

Inhibitor studies

The PPIase activity of PfCyP19 was examined for inhibition by CsA and a selection of analogues. At an enzyme concentration of 20 nM, an IC_{50} of 19.4 ± 1.8 nM was obtained for CsA (Figure 5). No time dependence of inhibition was observed with incubations between 5–60 min. The inhibition data were re-analysed to determine an apparent K_i of 6.9 ± 2.3 nM, and thus facilitate comparison with kinetic data from other CyPs, using a rearrangement of the Morrison equation [42] describing a tight binding competitive inhibitor as reported previously [41]:

$$\frac{k_i}{k_o} = \frac{-(K_{i,app} + i_T - E_T) + \sqrt{[(K_{i,app} + i_T - E_T)^2 + 4K_{i,app}E_T]}}{2E_T} \quad (1)$$

Where, $K_{i,app} = (S + K_m)K_i/K_m$, i_T and E_T are the total concentration of inhibitor and enzyme respectively and k_i is the enzymic rate constant in the presence of an inhibitor. The re-analysed data are shown superimposed on the IC_{50} curve for CsA (Figure 5, broken line). $K_{i,app}$ values for other inhibitors, based on median-dose experiments, were determined in the same way (Table 1). Of the 12 CsA analogues tested, ten of these inhibited PPIase activity with an IC_{50} in the range 14.2–39.6 nM ($K_{i,app}$ between 3.3 and 27.8 nM) and therefore represent strong inhibitors (Table 1). These ten compounds had one or more modifications at positions 1, 3, 4 and 8 in the undecapeptide ring of CsA (Figure 6), suggesting that a large number of ring substitutions are possible that maintain inhibition of PPIase activity. Notable exceptions were CsC (**2**) and CsD (**3**) (where the emboldened, underlined numbers relate to the compounds shown in Table 1), which have substitutions at the 2 position and markedly increased $K_{i,app}$ values. However, an additional substitution in **2** at the 1 position and at the 3 position in **3** produced inhibitors **5** and **6** respectively, with $K_{i,app}$ values comparable with CsA. Interestingly, the MeSer[3] substitution alone (**7**) had no effect on the $K_{i,app}$ relative to that of CsA. Additional substitution with D-Ile at the 4 position in **8** had no effect on the $K_{i,app}$, but a substitution of MeVal at the 4 position in **1** and **7** produced inhibitors **10** and **9**, respectively, with slightly reduced PPIase inhibition. Other changes including saturation of the side chain in

Table 1 Inhibition of PfCyP19 PPIase activity and *P. falciparum* growth *in vitro* by CsA analogues

The method used is described in the Materials and methods section. The data of Bell et al. [26] for parasite growth inhibition are shown in parentheses. Abu, aminobutyric acid.

Compound	PPIase inhibition		Parasite inhibition
	IC_{50} (nM)	$K_{i,app}$ (nM)	EC_{50} (nM)
1 [Abu[2]]-Cs (CsA)	19.4 ± 1.8	6.9 ± 2.0	210 ± 23 (300)
2 [Thr[2]]-Cs (CsC)	581 ± 112	690 ± 347	120 ± 11
3 [Val[2]]-Cs (CsD)	238 ± 36	218 ± 46.8	700 ± 330 (260)
4 [Dihydro-MeBmt[1]]-CsA	28.9 ± 3.0	10.7 ± 4.1	180 ± 38
5 [(8′-OMe)dihydro-MeBmt[1]]-CsC	27.2 ± 1.7	13.2 ± 7.4	540 ± 120
6 [D-MeSer[3]]-CsD	17.6 ± 3.8	6.8 ± 2.2	2250 ± 180
7 [D-MeSer[3]]-CsA	19.7 ± 1.0	6.7 ± 3.8	890 ± 24 (970)
8 [D-MeSer[3]][D-Ile[4]]-CsA	19.7 ± 1.0	7.4 ± 2.1	2370 ± 190
9 [D-MeSer[3]][MeVal[4]]-CsA	32.0 ± 2.8	13.6 ± 4.5	2060 ± 190
10 [MeVal[4]]-CsA	27.7 ± 2.3	14.4 ± 7.2	1040 ± 100 (330)
11 [D-Ser[8]]-CsA	39.6 ± 5.4	27.8 ± 8.9	360 ± 57
12 [(2-Hydroxyethoxy)-D-Ser[8]]-CsA	21.9 ± 1.3	14.0 ± 4.6	410 ± 39
13 [(2-Aminoethoxy)-D-Ser[8]]-CsA-[D-Ser[8]-OAc]-CsA-N-amide	14.2 ± 1.5	3.3 ± 1.1	300 ± 17
14 Rapamycin	> 5000		2690 ± 350 (2600)
15 FK506	> 10000		2070 ± 100 (1900)

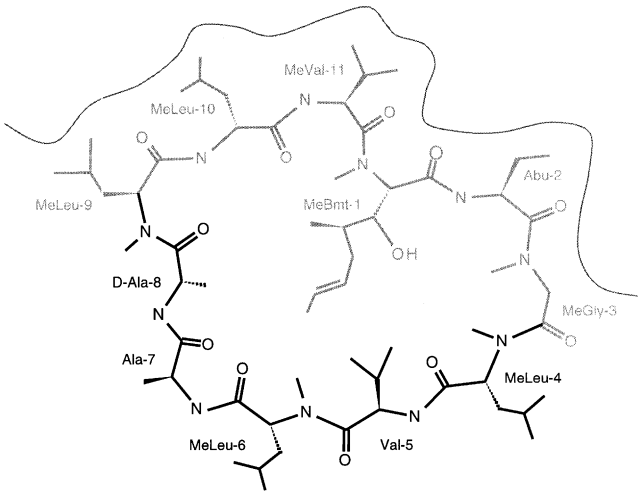

Figure 6 Chemical structure of CsA in its CyP-bound conformation

The line represents the CsA binding pocket, as found in the hCyPA–CsA complex, and CsA residues that comprise part of the 'effector surface' are highlighted.

dihydro-MeBmt[1] (4-[(*E*)-2-butenyl]-4,*N*-dimethyl-L-threonine) CsA (**4**) and substitutions at position 8 in **11** and **12** caused a slight increase in relative $K_{i,app}$ values. Only one analogue (**13**) showed greater inhibition than CsA, with a $K_{i,app}$ that was approx. half that of the parent compound. The compound is a CsA dimer bridged via the side chain at position 8. A possible explanation for the strong inhibition by this analogue may be an ability to bind 2 CyP molecules simultaneously. Rapamycin (**14**) and FK506 (**15**) are inhibitors of the FKBP (FK506 binding protein) family of PPIases and, as expected, were inactive as CyP inhibitors. Inhibition of parasite growth *in vitro* was also examined for CsA (Figure 5) and its analogues, in addition to FK506 and rapamycin (Table 1). Under the conditions used, CsA had an EC_{50} of 210 ± 23 nM. Both CsC (**2**) and dihydro-MeBmt[1]-CsA (**4**) showed marginally greater inhibition than CsA. All the other CsA analogues inhibited parasite growth, although compounds **6**–**10** with substitutions at the 3 and/or 4 positions decreased antimalarial activity by 2.5- to 10-fold. Previously reported EC_{50} values for six of the inhibitors [26] are in broad agreement with values found in the present study, with the exception of MeVal[4]-CsA (**10**) which in the present assay system had a significantly higher EC_{50} than CsA. Consistently with the previous report [26], we found no correlation between inhibition of PPIase activity and parasite growth.

It has been reported that CsA may be involved in reversing resistance to the antimalarial drug, chloroquine [43]. Of the antimalarials amodiaquine, artemesinin, chloroquine, primaquine, quinacrine and quinine, none inhibited PPIase activity at a concentration of 10 μM. Haemin, the putative primary receptor for chloroquine [44], inhibited PPIase activity with an IC_{50} of 8.9 ± 2.1 μM. Inhibition by 10 μM haemin was not affected by the presence of an equimolar amount of chloroquine. Thus PfCyP19 is unlikely to be involved in chloroquine resistance by sequestering chloroquine or a chloroquine–haemin complex.

DISCUSSION

The first step in the development of a new lead drug against malaria, based on CsA, is the identification and characterization of the primary receptor of CsA. Toward this goal, we have identified a third member of a CyP family in *P. falciparum*, the properties of which are compared with the two described previously, *P. falciparum* CyPs and human CyPA (Table 2). A striking difference between PfCyP19 and the two other CyPs from *P. falciparum* is that it has no N-terminal extension. PfCyP24 has a long N-terminal sequence extension of unknown function and PfCyP22 has a cleavable signal sequence. These modifications may lead to the targetting of CyPs to different subcellular compartments in the malaria parasite, such as the mitochondrion, endoplasmic reticulum or the putative novel organelle, the apicoplast. The organellar localizations of specific CyPs have been reported in several organisms, including yeast [45] and mammalian cells [46]. An alignment of PfCyP19 with other CyPs revealed that, among the human CyPs, hCyPA was the closest human homologue. Human CyPA was originally identified as the cytosolic receptor for CsA mediating immunosuppression in T cells [1]. However, in malaria cells CsA is dispersed throughout the food vacuole and cytosol [43], and thus the antimalarial activity may be mediated by one or more CyPs in these subcellular localizations.

As expected from the sequence alignment, PfCyP19 is indeed an active PPIase, catalysing the *cis*/*trans* isomerization of suc-AAPF-pNA with a k_{cat}/K_m of 1.2×10^7 $s^{-1} \cdot M^{-1}$ (at 10 °C). This value is somewhat higher than that of PfCyP22 (2.3×10^6 $s^{-1} \cdot M^{-1}$, at 0 °C) [27], which is closer to the endoplasmic-reticulum-targeted hCyPB ($k_{cat}/K_m = 6.3 \times 10^6$ $s^{-1} \cdot M^{-1}$, at 10 °C [47]), but is very similar to that of 1.4×10^7 to 2.2×10^7 $s^{-1} \cdot M^{-1}$ determined for hCyPA [40,41]. The similarity between all of the specificity constants is consistent with the conservation of all 12 residues that interact with the substrate in the hCyPA crystal structure [38] (Figure 1).

In addition to the PPIase activity, PfCyP19 has a high affinity for CsA ($K_d = 13$ nM) and is therefore correctly termed a CyP

Table 2 Biochemical properties of the *P. falciparum* CyPs and human CyPA

The preprotein M_r for PfCyP22 and PfCyP24 was 21 700 and 24 000 respectively. For IC_{50} values the protein concentration (nM) is shown in parentheses. * Calculated assuming $IC_{50} = K_i + E_T/2$. nd, not determined.

					CsA binding		
CyP	M_r	N-terminal extension	K_m (μM)	k_{cat}/K_m ($\mu M^{-1} \cdot s^{-1}$)	K_d (nM)	IC_{50} (nM)	K_i (nM)
PfCyP19	19 000	None	$\gg 120$	12 ± 1	13 ± 2.7	19.4 ± 2.8 (20)	6.9 ± 2.3
PfCyP22	19 200	Putative ER targetting	nd	2.3	nd	10 (15)	2.5*
PfCyP24	19 500	Unknown function	nd	nd	nd	nd	nd
hCyPA	17 900	None	870 ± 84 [39]	14–22 [40,41]	200–360 [1,48]	6.6 (6) [32]	1.3–3.0 [2,41]

according to the formal definition, namely, a CsA binding protein. The K_d value determined in the present study is significantly lower than those determined for other CyPs, 200 nM for bovine [1] and 360 nM for recombinant hCyPA [48]. A previous calculation of a K_d of 46 nM for recombinant human CyP [40] did not consider the effect of CyP–CsA complex formation on the concentration of free CsA; these data have since been re-analysed and an increased K_d of 240 nM was found [48]. The PPIase activity of PfCyP19 was potently inhibited by CsA with an IC_{50} of 19.4 nM and an apparent K_i of 6.9 nM, which was similar to the human enzyme and compatible with the total conservation of residues involved in binding CsA (Figure 1). Within experimental errors, the $K_{i,app}$ and K_d were not markedly different, which is consistent with a model whereby both parameters describe the equilibrium dissociation constant of a simple CyP–CsA complex.

Several CsA analogues were tested both for inhibition of PPIase activity and parasite growth. With the exception of CsC and CsD, PPIase inhibition was largely the same for all of the CsA analogues. Furthermore, in common with another study [26], which examined PPIase activity in total malarial extracts, we failed to demonstrate a correlation between the anti-malarial activities and anti-PPIase activities of various analogues. However this lack of correlation does not mean that PfCyP19 can be discounted as the drug target. In T cells, the immunosuppressive activity of CsA is not because of the drug alone. Rather, a composite 'effector surface', comprising elements from hCyPA and CsA (Figure 6), is responsible for the inhibition of calcineurin (CN). Residues 4–8 of CsA contribute to the effector surface for CsA binding to CN, whereas the remaining six residues represent the 'ligand surface' in the binding pocket ('receptor surface') of the human enzyme [49]. This may also be the case for the malaria enzyme, since purified PfCyP19 complexed with CsA inhibits CN-like phosphatase activity in extracts of *P. falciparum* (personal communication, Dr. S. Barik).

The fact that CsC and CsD show markedly lower inhibition of PPIase activity, is consistent with residue 2 being important for CsA binding to PfCyP19. In hCyPA, the aminobutyric acid side chain of CsA is bound in a tight pocket formed by residues that are totally conserved in PfCyP19 (i.e. G79, A108, N109; see Figure 1) [49]. The potent antimalarial activity of the compounds may be an indication that weaker binding CsA analogues are nonetheless capable of forming sufficient PfCyP19–drug complex to sequester the target effector molecule (e.g. malaria CN). A striking feature of our data is the marked lowering of antimalarial activity with analogues that are modified at positions 3 and 4. We propose that these residues play an important part in a putative effector surface of a malarial CyP–CsA complex. In the human CyPA–CsA complex, residue 3 of CsA is located at the edge of the CsA binding pocket but, in PfCyP19, this residue may be more available for interactions with CN or other downstream targets because of slight alterations in the architecture of the binding site. Structural studies of a PfCyP19–CsA complex are underway to confirm this prediction. Even extreme alterations at the 8 position in CsA, such as the CsA dimer (**13**), have little effect on the antimalarial activity of the CsA analogues, suggesting a marginal involvement of side chains at this position in a putative *Plasmodium* effector surface.

These considerations suggest that PfCyP19 is a good candidate receptor for CsA in the malaria parasite. However, at the present time, it cannot be discounted that the other malarial CyPs or alternative targets, such as P-glycoprotein, are also involved [50]. Studies on the subcellular localization of the various PfCyPs, the mechanisms of acquiring resistance to CsA and CyP knockouts should help to clarify these predictions.

We thank Dr. K. Smith for his help in making the PCR probe used for cDNA library screening, Professor D. M. J. Lilley for the use of his fluorescence spectrophotometer and Dr. B. J. Berger for his advice on protein chromatography. This work was supported by a studentship (to M.B.) from the Medical Research Council. A.H.F. is supported by the Wellcome Trust (042368/067).

REFERENCES

1 Handschumacher, R. E., Harding, M. W., Rice, J., Drugge, R. J. and Speicher, D. W. (1984) Science **226**, 544–547
2 Fischer, G., Wittmann-Liebold, B., Lang, K., Kiefhaber, T. and Schmid, F. X. (1989) Nature (London) **337**, 476–478
3 Takahashi, N., Hayano, T. and Suzuki, M. (1989) Nature (London) **337**, 473–475
4 Fischer, G., Bang, H. and Mech, C. (1984) Biomed. Biochim. Acta **43**, 1101–1111
5 Galat, A. (1993) Eur. J. Biochem. **216**, 689–707
6 Baker, E. K., Colley, N. J. and Zuker, C. S. (1994) EMBO J. **13**, 4886–4895
7 Ferreira, P. A., Nakayama, T. A. and Travis, G. H. (1997) Proc. Natl. Acad. Sci. U.S.A. **94**, 1556–1561
8 Freskgård, P. O., Bergenhem, N., Jonsson, B. H., Svensson, M. and Carlsson, U. (1992) Science **258**, 466–468
9 Kern, G., Kern, D., Schmid, F. X. and Fischer, G. (1994) FEBS Lett. **348**, 145–148
10 Ratajczak, T., Carello, A., Mark, P. J., Warner, B. J., Simpson, R. J., Moritz, R. L. and House, A. K. (1993) J. Biol. Chem. **268**, 13187–13192
11 Kieffer, L. J., Seng, T. W., Li, W., Osterman, D. G., Handschumacher, R. E. and Bayney, R. M. (1993) J. Biol. Chem. **268**, 12303–12310
12 Gamble, T. R., Vajdos, F. F., Yoo, S., Worthylake, D. K., Houseweart, M., Sundquist, W. I. and Hill, C. P. (1996) Cell **87**, 1285–1294
13 Sherry, B., Zybarth, G., Alfano, M., Dubrovsky, L., Mitchell, R., Rich, D., Ulrich, P., Bucala, R., Cerami, A. and Bukrinsky, M. (1998) Proc. Natl. Acad. Sci. U.S.A. **95**, 1758–1763
14 Dolinski, K., Muir, S., Cardenas, M. and Heitman, J. (1997) Proc. Natl. Acad. Sci. U.S.A. **94**, 13093–13098
15 Davis, E. S., Becker, A., Heitman, J., Hall, M. N. and Brennan, M. B. (1992) Proc. Natl. Acad. Sci. U.S.A. **89**, 11169–11173
16 Duina, A. A., Marsh, J. A. and Gaber, R. F. (1996) Yeast **12**, 943–952
17 Oliver, S. G., Van Der Aart, Q. J. M., Agostoni-Carbone, M. L., Aigle, M., Alberghina, L., Alexandraki, D., Antoine, G., Anwar, R., Ballesta, J. P. G., Benit, P. et al. (1992) Nature (London) **357**, 38–46
18 Breuder, T., Hemenway, C. S., Movva, N. R., Cardenas, M. E. and Heitman, J. (1994) Proc. Natl. Acad. Sci. U.S.A. **91**, 5372–5376
19 Liu, J., Farmer, Jr., J. D., Lane, W. S., Friedman, J., Weissman, I. and Schreiber, S. L. (1991) Cell **66**, 807–815
20 Beals, C. R., Clipstone, N. A., Ho, S. N. and Crabtree, G. R. (1997) Genes Dev. **11**, 824–834
21 High, K. P. and Handschumacher, R. E. (1995) Infect. Agents Dis. **1**, 121–135
22 Thommen-Scott, K. (1981) Agents Actions **11**, 770–773
23 Nickell, S. P., Scheibel, L. W. and Cole, G. A. (1982) Infect. Immun. **37**, 1093–1100
24 Kocken, C. H. M., Van Der Wel, A., Rosenwirth, B. and Thomas, A. W. (1996) Exp. Parasitol. **84**, 439–443
25 Chappell, L. H. and Wastling, J. M. (1993) Parasitology **107**, S25–S40
26 Bell, A., Wernli, B. and Franklin, R. M. (1994) Biochem. Pharmacol. **48**, 495–503
27 Hirtzlin, J., Farber, P. M., Franklin, R. M. and Bell, A. (1995) Eur. J. Biochem. **232**, 765–772
28 Reddy, G. R. (1995) Mol. Biochem. Parasitol. **73**, 111–121
29 Trager, W. and Jensen, J. B. (1976) Nature (London) **193**, 673–675
30 Sambrook, J., Fritsch, E. F. and Maniatis, T. (1989) Molecular Cloning: A Laboratory Manual, 2nd edn., Cold Spring Harbor Laboratory Press, Cold Spring Harbor, NY
31 Bose, S., Mucke, M. and Freedman, R. B. (1994) Biochem. J. **300**, 871–875
32 Liu, J., Chen, C. M. and Walsh, C. T. (1991) Biochemistry **30**, 2306–2310
33 Makler, M. T. and Hinrichs, D. J. (1993) Am. J. Trop. Med. Hyg. **48**, 205–210
34 Knobloch, J. and Henk, M. (1995) Trans. R. Soc. Trop. Med. Hyg. **89**, 269–270
35 Weber, J. L. (1988) Exp. Parasitol. **66**, 143–170
36 Fischer, G. (1994) Angew. Chem. Int. Ed. Engl. **33**, 1415–1436
37 Pflugl, G., Kallen, J., Schirmer, T., Jansonius, J. N., Zurini, M. G. M. and Walkinshaw, M. D. (1993) Nature (London) **361**, 91–94
38 Zhao, Y. and Ke, H. (1996) Biochemistry **35**, 7356–7361
39 Kofron, J. L., Kuzmic, P., Kishore, V., Colón-Bonilla, E. and Rich, D. H. (1991) Biochemistry **30**, 6127–6134
40 Liu, J., Albers, M. W., Chen, C., Schreiber, S. L. and Walsh, C. T. (1990) Proc. Natl. Acad. Sci. U.S.A. **87**, 2304–2308
41 Bergsma, D. J., Eder, C., Gross, M., Kersten, H., Sylvester, D., Appelbaum, E., Cusimano, D., Livi, G. P., McLaughlin, M. M., Kasyan, K. et al. (1991) J. Biol. Chem. **266**, 23204–23214

42 Henderson, P. J. F. (1972) Biochem. J. **127**, 321–333
43 Scheibel, L. W., Colombani, P. M., Hess, A. D., Aikawa, M., Atkinson, C. T. and Milhous, W. K. (1987) Proc. Natl. Acad. Sci. U.S.A. **84**, 7310–7314
44 Francis, S. E., Sullivan, Jr., D. J. and Goldberg, D. E. (1997) Annu. Rev. Microbiol. **51**, 97–123
45 Dhillon, N. and Thorner, J. (1996) Methods: A Companion to Methods in Enzymology **9**, 165–176
46 Fruman, D. A., Burakoff, S. J. and Bierer, B. E. (1994) FASEB J. **8**, 391–400
47 Price, E. R., Zydowsky, L. D., Jin, M. J., Baker, C. H., McKeon, F. D. and Walsh, C. T. (1991) Proc. Natl. Acad. Sci. U.S.A. **88**, 1903–1907
48 Holzman, T. F., Egan, D. A., Edalji, R., Simmer, R. L., Helfrich, R., Taylor, A. and Burres, N. S. (1991) J. Biol. Chem. **266**, 2474–2479
49 Taylor, P., Husi, H., Kontopidis, G. and Walkinshaw, M. D. (1997) Prog. Biophys. Mol. Biol. **67**, 155–181
50 Silverman, J. A., Hayes, M. L., Luft, B. J. and Joiner, K. A. (1997) Antimicrob. Agents Chemother. **41**, 1859–1866

Received 5 May 1998/12 June 1998; accepted July 6 1998